

## Structural and optical properties of nanocrystalline tin sulphide thin films deposited by thermal evaporation

A Salem<sup>1,2</sup>, S S Ahmed<sup>1,2</sup> & S N Alamri<sup>3</sup>

<sup>1</sup>Physics Department, Faculty of Science, South Valley University, Qena, Egypt

<sup>2</sup>Physics Department, Faculty of Science, King Khalid University, Abha, Saudia Arabia Kingdom

<sup>3</sup>Department of Physics, Faculty of Education, Taibah University, Saudia Arabia Kingdom

\*E-mail: salemabouelwafa@yahoo.co.uk(Abouelwafasalem)

Received 20 August 2013; revised 8 January 2015; accepted 29 June 2015

Thermal evaporation technique was used to fabricate the nanocrystalline tin sulphide (SnS) thin films of thicknesses 200 and 377 nm on good quality glass substrate. The various physical properties of deposited thin films have been investigated using X-ray diffraction (XRD), Atomic force microscopy (AFM), and ultraviolet-visible-near infrared spectroscopy at room temperature. X-ray diffraction analysis confirmed the orthorhombic phase of SnS films and the calculated lattice parameters have been calculated. The grain size, dislocation density and micro strain have been calculated using X-ray data. The result from AFM analysis shows that the surface of films was compact, dense and smooth. The optical band gap and types of transitions involved in the absorption process have been investigated. For allowed direct and indirect transition, the band gap values varied in the range 1.96-1.72 eV and 1.58-0.92 eV, respectively. The deduced values of the band gap suggest that the deposited thin films can be used in the fabrication of solar cell devices.

**Keywords:** Thin films, Vapour deposition, Atomic force microscopy, X-ray diffraction, Optical properties

### 1 Introduction

The search for thin film materials for solar energy conversion and other related applications has been of great interest in recent past. Many efforts have been made towards using metal chalcogenides as this class of materials which shows somewhat superior performance as compared to others.

Among the important binary semiconductors of IV-VI group, the chalcogenides formed with Sn, especially tin sulphide compounds (SnS) have attracted considerable attention because of their physical properties, which are suitable for optoelectronic devices. SnS has particularly generated interest because of its non-toxic nature and absorption tunable band gap in the visible range. SnS thin films was prepared by various methods such as plasma enhanced chemical vapour deposition (PECVD), vacuum evaporation, chemical bath deposition, electrodeposition, and spray pyrolysis<sup>1-11</sup> with the purpose of manufacturing thin films suitable for using as solar absorber in photovoltaic applications.

Due to the increasing interest of SnS, the ways of growing good quality SnS thin films with better properties for photovoltaic and solar cell applications using thermal evaporation under vacuum and

controlled deposition conditions with attention given to its structural and optical properties, have been investigated in the present paper. The physical properties of the SnS thin films deposited by thermal evaporation have been studied.

### 2 Experimental Details

The compound was prepared as a block compound by using Bridgman-Stockbarger method. In this method, the ampoule charged with required amount of pure tin (Aldrich Mark 99.999%) and pure sulphur (Aldrich Mark 99.999%) according to the atomic weight of compound. After the compound SnS prepared as polycrystalline compound, thermally evaporated to have thin film samples. Thin films of SnS were deposited by thermal evaporation using molybdenum boat on glass substrates at room temperature with thickness 200 and 377 nm. The thicknesses of the films were measured with a Dektak 150 surface profiler. Structural properties of tin sulphide films were studied by X-ray diffraction (XRD) using a diffractometer Shimadzu 6000 (XRD-6000) with a CuK $\alpha$  line ( $\lambda=1.5405 \text{ \AA}$ ) with  $2\theta$  ranging from  $5^\circ$  to  $90^\circ$ . The X-ray tube voltage and current were 40 kV and 30 mA, respectively. The speed of the detector was  $1^\circ$  per min.

The surface morphology of the deposited films was examined using atomic force microscopy (AFM, Veeco CP-II) in non-contact mode with Si tips at a scan rate of 1 Hz (AFM image for 377 nm thin film). The transmittance,  $T(\lambda)$ , and reflectance,  $R(\lambda)$  spectra of the deposited films were measured at a normal and  $5^\circ$  incident angle, respectively. These measurements were acquired in air at room temperature using a computer-aided double beam spectrophotometer (Shimadzu 3150 UV-Vis-NIR). The absorption coefficient ( $\lambda$ ) was calculated from  $T(\lambda)$  and  $R(\lambda)$  measurements and from its dependence on the photon energy ( $h\nu$ ), The optical band gap  $E_g$  was obtained.

### 3 Results and Discussion

#### 3.1 Morphology and Structural Analysis

Figure 1 shows the recorded XRD pattern of the deposited SnS thin film prepared on glass substrate at room temperature. All reflections can be indexed to pure orthorhombic SnS phase as compared with the JCDPS 83-1758 with no impurities peaks such as elemental tin, sulphur and other tin sulphide phases, indicating the formation of single phase SnS. The  $2\theta$  peaks observed at  $31.4^\circ$ ,  $39.0^\circ$ ,  $42.96^\circ$ ,  $51.36^\circ$ , and  $54.62^\circ$  exhibit the formation of the orthorhombic phase of SnS which correspond to the (111), (131), (002), (151), and (042) planes of reflections. The strongest peak for the grown films in Fig. 1 occurred at  $2\theta = 31.4^\circ$  with  $d = 2.851 \text{ \AA}$  which corresponds to (111). The different peaks in the diffractogram were indexed and the corresponding values of inter-planar spacing  $d$  were calculated and compared with the standard values<sup>12</sup> JCPDS Diffraction Data Card No.

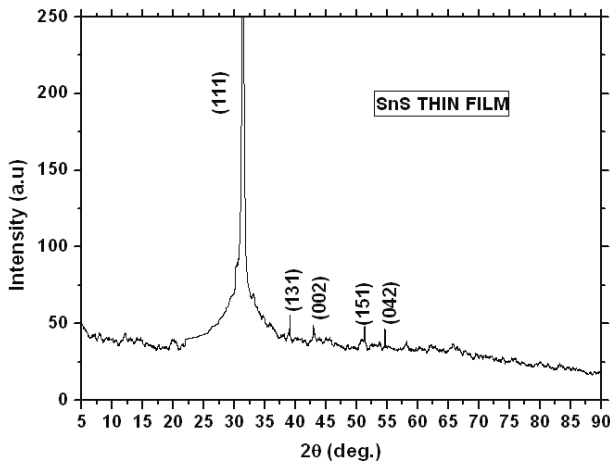


Fig. 1 — XRD pattern of the SnS films

89-0253. The inter-planar distances as indicated in the XRD result were found to be 2.69, 4.178, 2.553 and 2.627  $\text{\AA}$ . The presence of the large number of peaks indicates that the film is polycrystalline in nature and good crystalline structure because of sharp structural peaks. From X-ray diffraction data, the crystallite size of the deposited film was calculated using Debye-Scherrer formula<sup>12</sup>. The Miller indices ( $hkl$ ) relate the interplanar distance  $d_{hkl}$  or  $d$ -spacings to the lattice parameters by an equation specific to the crystal system. For example, in a structure with an orthorhombic unit cell the relationship<sup>13</sup> is given by:

$$\frac{1}{d_{hkl}^2} = \frac{h^2}{a^2} + \frac{k^2}{b^2} + \frac{l^2}{c^2} \quad \dots(1)$$

According to the data of the XRD peaks, the lattice parameters ( $a$ ,  $b$  and  $c$ ) of the SnS film have been calculated. The evaluated lattice parameters of the SnS film<sup>14</sup> are  $a = 4.148 \text{ \AA}$ ,  $b = 11.48 \text{ \AA}$ , and  $c = 4.177 \text{ \AA}$ , the broadening of peaks of XRD pattern is inversely proportional to the average crystallite size ( $D$ ):

$$D = \frac{K\lambda}{\beta \cos \theta} \quad \dots(2)$$

where  $D$  is the grain size,  $\lambda$  is the wavelength of the  $\text{CuK}\alpha$  radiation used ( $\lambda = 1.5405 \text{ \AA}$ ),  $K$  is a constant<sup>15</sup> generally taken to have the value 0.9,  $\beta$  is the full width at half maximum FWHM of the reflection peak that has the same maximum intensity in the diffraction pattern and  $\theta$  is the diffraction angle of x-rays.

For the fabrication of good quality thin film to use in optical devices, it is necessary to reduce the surface roughness and dislocation density of the SnS film. So the value of the dislocation density ( $\delta$ ) which gives the number of defects in the film was calculated from the average values of the crystallite size  $D$  by the Williamson and Smallman's formula<sup>16</sup>:

$$\delta = \frac{1}{D^2} \quad \text{lines/m}^2 \quad \dots(3)$$

The micro strain ( $\varepsilon$ ) is obtained using the relation:

$$\varepsilon = \frac{\beta \cos \theta}{4} \quad \dots(4)$$

Table 1 — Plane (*hkl*), FWHM value, grain size (*D*), dislocation density ( $\delta$ ), and the micro strain ( $\epsilon$ ) values of SnS thin film

$2\theta$ (degree)	<i>d</i> Å (spacing)	$\beta$ (FWHM)	<i>hkl</i>	Grain Size ( <i>D</i> ) Nm	Density ( $\delta$ ) $\times 10^{13}$ Lines/m <sup>2</sup>	Micro strain ( $\epsilon$ ) $\times 10^{-5}$
31.4	2.851	0.5	111	16.6	360	210
39.0	2.332	0.11	131	84	14	45
42.96	2.089	0.12	002	214	2.18	49
51.36	1.346	0.114	151	71.4	19.6	37
54.6	1.689	0.123	042	71.8	19.4	8

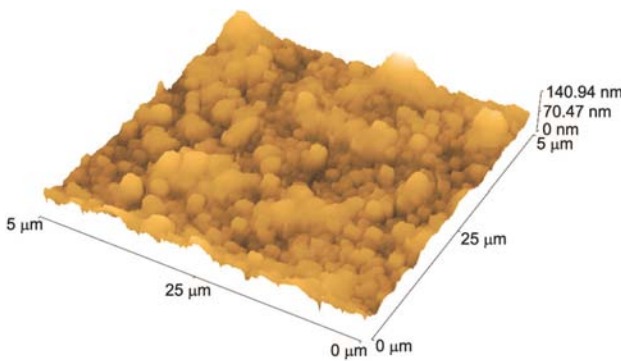


Fig. 2 — AFM image for 377 nm thin film

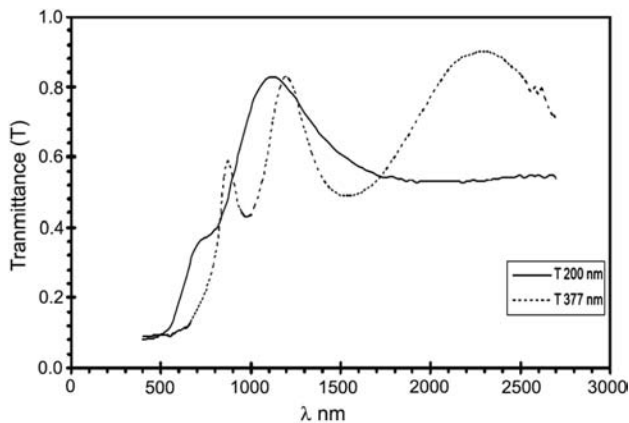


Fig. 3 — Transmission spectra (*T*) of SnS thin films

All these parameters, the (*hkl*) plane, FWHM value, grain size (*D*), dislocation density ( $\delta$ ) and the micro strain ( $\epsilon$ ) values of SnS thin film are calculated and presented in Table 1. Figure 2 shows the AFM image of the SnS thin film (AFM image for 377 nm thin film), the mean roughness of SnS surfaces was approximately 10.8 nm. The value of the roughness was calculated by the program of the instrument.

**3.2 Optical Properties**

Optical properties are very important for solar cell materials. Figure 3 shows the optical transmission spectra *T*( $\lambda$ ) for SnS thin films of thickness 200 and 377 nm in the wavelength range 400-1200 nm.

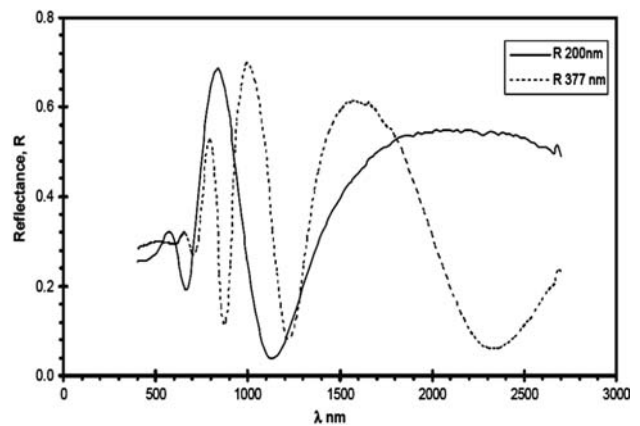


Fig. 4 — Reflection spectra (*T*) of SnS thin films

Figure 4 shows the optical reflection *R*( $\lambda$ ) spectra for SnS thin films of thickness 200 and 377 nm in the wavelength range 400-1200 nm. The transmission *T*( $\lambda$ ) through an absorbing slab is related to its reflectivity *R*( $\lambda$ ), thickness *d* and the absorption coefficient  $\alpha$  by:

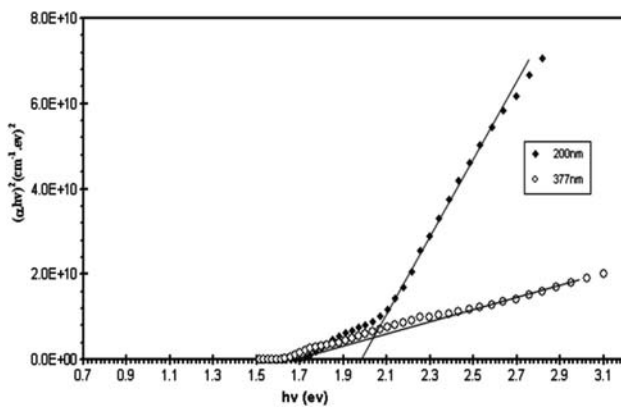
$$T = (1 - R) \exp - \alpha d \quad \dots(5)$$

In order to estimate the optical band gap, the following equation can be used:

$$(\alpha h\nu) = A(h\nu - E_g)^n \quad \dots(6)$$

where  $E_g$  is the energy band,  $\alpha$  the absorption coefficient, *A* is a constant and *n* characterizes the transition process which has values  $n = 1/2$  and  $3/2$  for direct allowed and forbidden transitions, respectively.  $n = 2$  and  $3$  for indirect allowed and forbidden transitions, respectively.

Figure 5 shows the plot of  $(\alpha h\nu)^2$  versus photon energy for SnS thin films of thickness 200 and 377 nm, respectively. Each curve tends to a straight line in the high photon energy region (Fig. 5). By extrapolating the straight line from this linear region,  $E_g$  was estimated by the intercept with the energy axis.

Fig. 5 —  $(\alpha hv)^2$  versus  $hv$  of SnS thin films

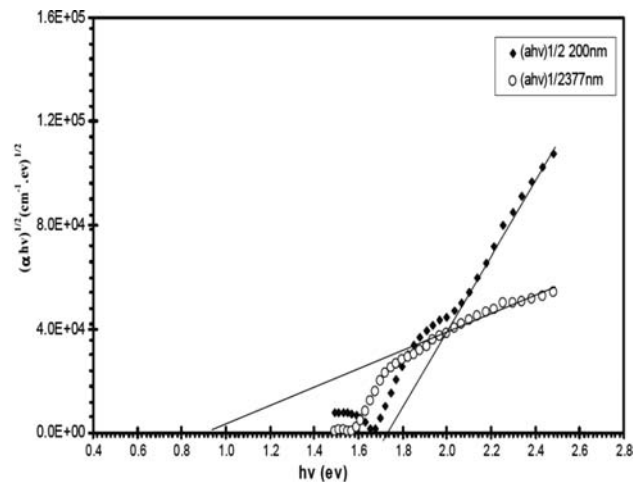
The values of the direct allowed transition for both thickness 200, 377 nm is 1.96 and 1.58 eV, respectively. The thinner (200 nm) has a large direct band gap of 1.96 eV (Fig. 5). Because of use of very thin films results in larger transmission in the shorter wavelength, this agrees well with Ref. (17). To calculate the wavelength corresponding to direct band gap using the Eq.  $E = h\nu$  where  $h$  is Planck constant and  $\nu$  frequency  $E = hc/e\lambda e$  electron charge,  $c$  speed of light and  $\lambda$  wavelength,  $E_{\text{energy}}$ , so:

$$\begin{aligned}\lambda &= hc/eE = 6.6 \times 10^{-34} \times 3 \times 10^8 / 1.6 \times 10^{-19} \times 1.96 \\ \lambda &= 6.313 \times 10^{-7} \text{ m} \\ \lambda &= 6.313 \times 10^{-7} \times 10^{10} = 6313 \text{ \AA}\end{aligned}$$

so this value in visible light spectrum range and for

$$\begin{aligned}E_g &= 1.58 \text{ eV} \\ \lambda &= 7.832 \times 10^{-7} \times 10^{10} = 7832 \text{ \AA}\end{aligned}$$

Figure 6 shows the plot of  $(\alpha hv)^{1/2}$  versus photon energy for SnS thin films of thickness 200 and 377 nm, respectively. The indirect band gap  $E_{\text{ind}}$  is often estimated by the intercept of the energy axis at  $(\alpha hv)^{1/2} = 0$ , it has the values of 1.72 and 0.92 eV for samples of thickness 200 and 377 nm, respectively. Table 2 presents the total values of direct and indirect energy gaps of the present work these values agree well with other published results reported by Guneri *et al.*<sup>18</sup>. in which band gap values varied in the range 1.3-1.97 eV for allowed direct transition and 0.83-1.36 eV for allowed indirect transition. The deduced values of the band gap in the present work are optimized values for the solar absorber in solar cell devices. The effect of different thicknesses in structure and optical properties of SnS, has been

Fig. 6 —  $(\alpha hv)^{1/2}$  versus  $hv$  of SnS thin films

studied in the present work. The reported direct and indirect optical band gap energies for SnS thin films varied in the range 1.2-2 eV and 0.8-1.2 eV, respectively<sup>19,20</sup>. Albers *et al.*<sup>21</sup>. reported indirect band gap of SnS single crystal is 1.07 eV, whereas it is 1.1 eV as reported by Nassary<sup>22</sup>.

#### 4 Conclusions

The nanocrystalline tin sulphide thin films with thicknesses 200 and 377 nm have been deposited on glass substrates at room temperature by thermal evaporation. Morphology and structure characterization of films have been investigated using AFM and XRD. The films exhibit SnS phase in crystalline in nature. The optical properties of SnS thin films of thickness 200 and 377 nm have been investigated. The films have two transition band gap direct and indirect band gap. These polycrystalline, single-phase and highly absorbing SnS thin films are suitable for the solar absorber in solar cell devices.

#### References

- 1 Thangaraju B & Kaliannam P, *J Phys D Appl Phys*, 33 (2000) 1054.
- 2 Reddy N Koteswara & Reddy K T Ramakrishna, *Thin Solid Films*, 325 (1998) 4.
- 3 Pramanik P, Basu P K & Biswas S, *Thin Solid Films*, 150 (1987) 269.
- 4 Zainal Z, Hussein M Z & Ghazali A, *Solar Energy Matter Solar Cells*, 40 (1996) 347.
- 5 Ghazali A, Zainal Z, Hussein M Z & Kasseim A, *Solar Energy Matter Solar Cells*, 55 (1998) 237.
- 6 Deraman K, Sakrani S, Ismail B B, Wahab Y & Gould R D, *Int J Electron*, 76 (1994) 917.

- 7 Ortiz A, Alonso J C, Garcia M & Toriz J, *Semicond Sci Technol*, 11 (1996) 243.
- 8 Ghosh B, Das M, Banerjee P & Das S, *Sol Energy Matter Sol Cells*, 92 (2008) 1099.
- 9 Avellaneda D, Nair M T S & Nair P K, *J Electrochem Soc*, 155 (2008) 525.
- 10 Sato N, Ichimura M, Arai E & Yamazaki Y, *Sol Energy Matter Sol Cells*, 85 (2005) 153.
- 11 Reddy K T R, Reddy N K & Miles R W, *Sol Energy Matter Sol Cells*, 90 (2006) 3041.
- 12 Cullity B D, In *Elements of X-ray diffraction* 2nd Edition, Addison Wesley, (1978).
- 13 Cullity B, *Elements of X-ray diffraction*, Addison-Wesley Publishing Company Inc., USA, (1967) 501.
- 14 Willeke G, Dasbach R, Sailer B & Bucher E, *Thin Solid Films*, 213 (1992) 271.
- 15 Jensen H, Pedersen J H, Jorgensen J E, Pedersen J Skov, Joensen K D, Iversen S B & Sogaard E G, *J of Experiem Nanosci*, 1 (2006) 355.
- 16 Williamson G B & Smallman R C, *Philos Mag*, 34 (1956) 46.
- 17 Devika M, Reddy N Koteeswara, Ramesh K, Ganesan R, Gu-nasekhar K R, Gopal E S R & Reddy K T Ramakrishna, *J Electrochem Soc*, 154 (2007) 67.
- 18 Guneri E, Ulutas C, Kirmizigul F, Altindemir G, Gode F & Gumus C, *Appl Surface Sci*, 257 (2010) 1189.
- 19 Lopez S & Ortiz A, *Semicond Sci Technol*, 9 (1994) 2130.
- 20 Devika M, Reddy N Koteeswara, Reddy D Sreekantha, Ahsanul-haq Q, Ramesh K, Gopal E S R, Gunasekhar K R, Hahn Y B, *J Electrochem Soc*, 155 (2008) 130.
- 21 Albers W, Haas C, Ober H, Schodder G R & Wasscher J D, *J Phys Chem Solids*, 23 (1962) 215.
- 22 Nassary M M, *J Alloys Compd*, 398 (2005) 21.